CHAPTER 3

FABRICATION AND CHARACTERIZATION OF SnO_2 NANOSTRUCTURES

In first chapter, it has been shown the various important applications of SnO_2, especially in advanced technology. Due to a good sensitivity and stability, the commercial gas sensors based on SnO_2 are available. To minimize the scale of devices, to reduce the power consumption, or to improve the gas sensor properties are reasons that many researches carry out fabrication of SnO_2 nanostructures.

Many techniques have been used to synthesize SnO_2 nanostructures, such as hydrothermal route, thermal evaporation, sol–gel template, or electrospining and atomic layer deposition. In hydrothermal route, tin dichloride or stannous chloride ($SnCl_2$) is used as starting material. $SnCl_2$ powder is commonly dissolved in alcohol solution. The solution is then gradually heated to about 150–400°C for formation of tin oxides. Various morphologies have been synthesized by using hydrothermal route, for example flower–like, prism–like, cubic–like, nanosheet, and hollow sphere SnO_2 nanostructures [66–69]. For thermal evaporation, the starting material can be Sn, SnO, or SnO_2. However, Sn and SnO are usually used because the process temperature is lower than that of SnO_2. The starting material is heated at high

temperature for oxidation and/or evaporation, under a carrier gas. The tin oxide vapor is then carried to crystallize on the substrate. Sn is oxidized rapidly at above 700°C and SnO is the initial form of the oxidation. Although the melting point of SnO is 1080°C, the vapor phase of SnO also occurs at low temperature. The SnO vapor can be carried to the substrate by carrier gas. SnO can decompose to SnO_2 at above 600°C due to the metastability of SnO. The decomposition of SnO leads to the formation of SnO_2 crystals. In the case using SnO_2 as a starting material, active carbon is employed to reduce evaporation temperature. In other word, the active carbon is used as thermal assistant. This technique is called "carbothermal reduction." SnO_2 nanowires and nanobelts are usually synthesized by using thermal evaporation method. The electrospining, atomic layer deposition [70] and sol gel–template [71] are usually used to synthesize SnO_2 nanotubes.

In this work, carbothermal reduction was used to fabricate SnO_2 nanostructures in a closed crucible by using SnO_2 powder as a starting material. This technique was shown to have an ability to fabricate various shapes of SnO_2 single crystal, for instances wire–like, belt–like, dendric–like, and cactus–like.

In this chapter, the fabrication of SnO_2 nanowires mixed nanodendrites and self–beaded nanowires will be discussed. Morphologies, growth direction, and crystal structure were observed by SEM, TEM, and XRD. The growth mechanism of these nanostructures will also be discussed.

3.1 Fabrication of SnO_2 nanostructures

SnO_2 powder (Aldrich, 99.9%) and carbon powder, with a weight ratio of 1:5, was mixed mechanically in a mortar for one hour. Then, 0.1g of the mixture was screened dispersedly at bottom of a crucible and Au–coated alumina substrates were placed in the crucible above the mixture, as shown in Fig 3.1. The crucible, closed with a lid, was placed into a horizontal alumina tubular furnace at room temperature. The furnace was heated to 850°C and kept at this temperature for an hour. Finally the crucible was moved out after the furnace was cooled down to room temperature. In the crucible, thick white wool–like layer covered over the surface of the alumina substrates. Moreover, belt–like and cactus–like microscale structures, were found on the crucible wall.

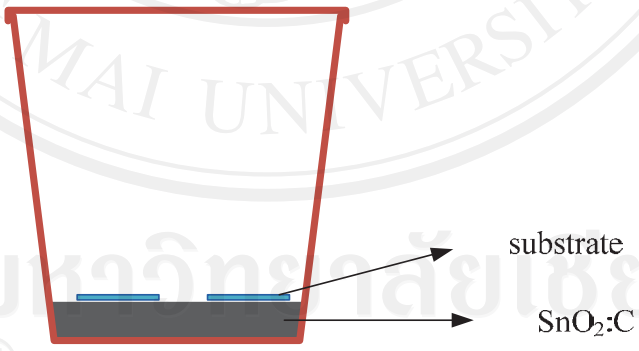

Figure 3.1 Crucible with SnO_2:C and gold–coated substrates

3.2 Characterization of SnO_2 nanostructures

3.2.1 SEM Characterization

There were many features of the as–synthesized SnO_2 products grown on the alumina substrates, as shown in Fig. 3.2. Each SEM image in Fig. 3.2 was taken from the SnO_2 product prepared with the same conditions but at different repeat. It revealed that the white wool products were based on SnO_2 nanowire structures. Fig. 3.2a shows the ultra long nanowires decorated with fuzzy branches. Fig. 3.2b and c show the ultra long nanowires beaded with particles. The SnO_2 nanowires with exiguous particle were found in some substrates as seen in Fig. 3.2d. The SnO_2 nanowires laid randomly on the substrate. The SnO_2 nanowires have diameter of 50 – 100 nm with only a few in the diameter up to 1μm and length of a few ten micrometers to hundred micrometers. These fuzzy branches could be called “nanodendrites” which are meandering chains with random branches. The size of the particles on parts of nanodendrites and beaded on the nanowires was about 100–300 nm and 300–1000 nm, respectively. It indicated that the nanowires were formed firstly and the nanodendrites come to attach on the nanowires later, as seen in Fig. 3.2a. In addition, it seemed that the particles formed at the same time with nanowires, as seen in Fig 3.2c. Moreover, in the case when the lid which covered the crucible was broken, microwires and cactus–like crystals were found on the wall of the crucible. A cactus–like crystal had spines around the backbone, as shown in Fig 3.3a. The diameter of the cactus–like crystals was about 50 μm. The higher magnification image, as seen in Fig. 3.3b, shows that the spines were similar to a leaf consisting aligned nanorods. The diameter of the nanorods was about 250 nm.

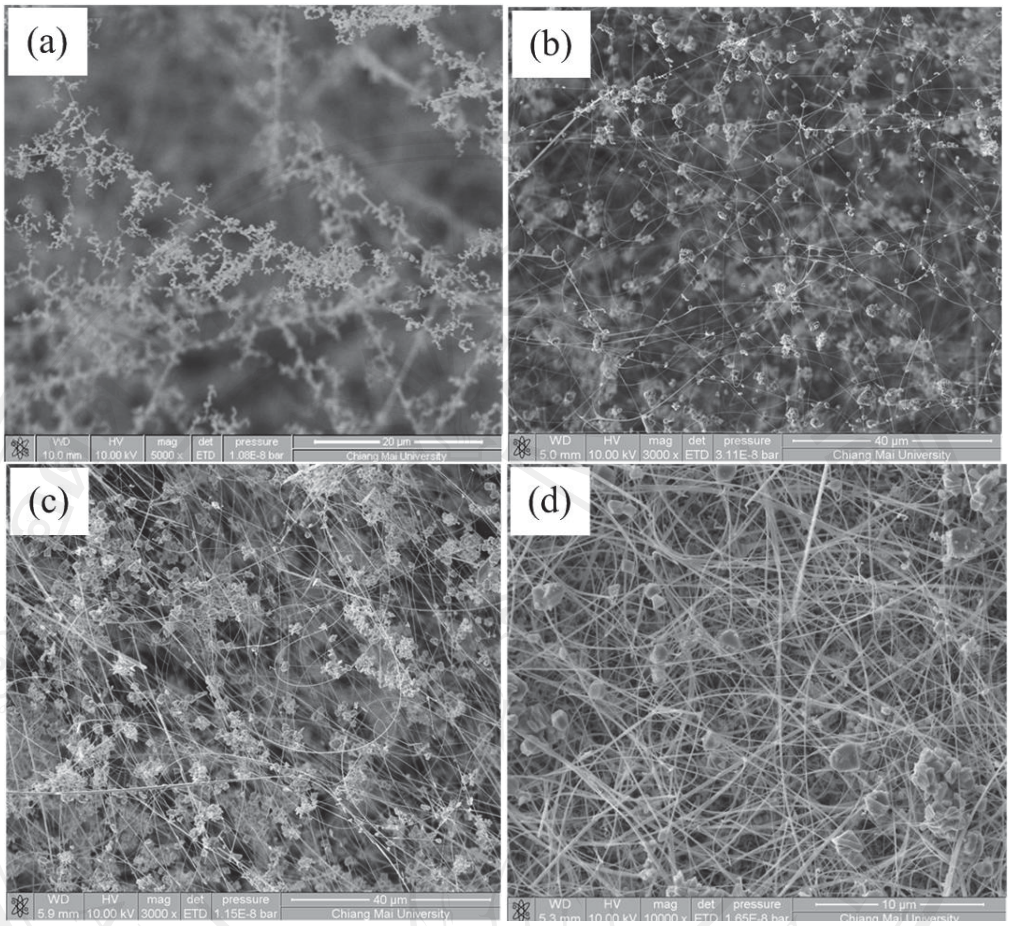

Figure 3.2 SEM images of the as–synthesized SnO_2 nanostructures four repeats: (a) nanowires decorated with nanodendrites, (b) – (c) nanowires beaded with particles (d) nanowires with exiguous particles.

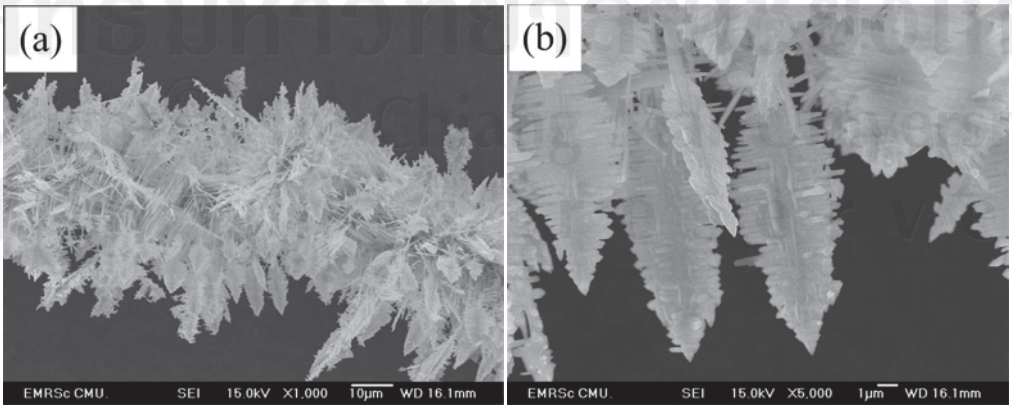

Figure 3.3 SEM images of cactus–like crystals: (a) trunk and (b) spines.

3.2.2 X–ray diffractometer

The XRD pattern of the SnO_2 nanostructures, taken from 20–80 degree of 2θ, is shown in Fig. 3.4. The pattern can be indexed according to the cassiterite structure of SnO_2 with lattice constants of a = 4.738 Å and c = 3.187 Å (JCPDS 41–1445) and the corundum structure of Al_2O_3 (JCPDS 42–1468) which comes from the substrate. No impurity or other structure phase was detected in the product. It means that the SnO_2 nanostructures were pure tetragonal rutile structure.

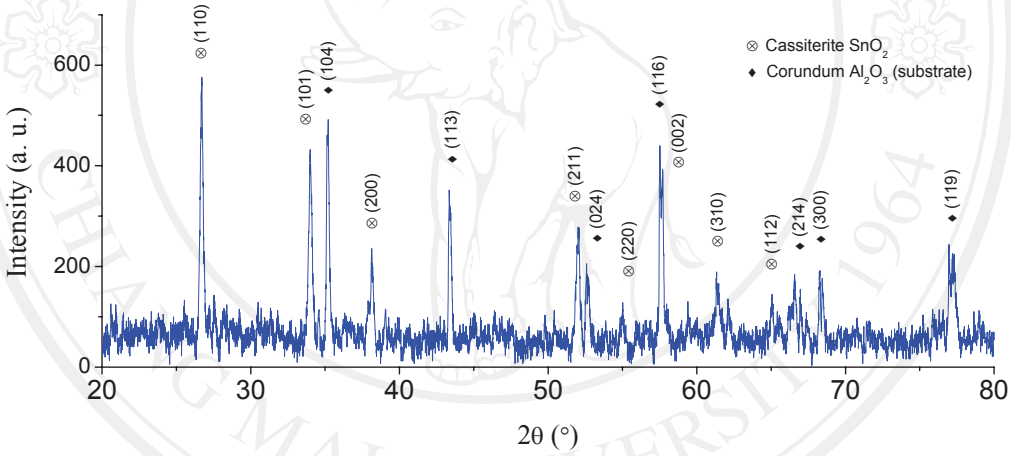

Figure 3.4 XRD profile of the SnO_2 nanostructures.

3.2.3 TEM characterization

The products were further analyzed using TEM and selected area electron diffraction (SAED). Fig. 3.5a shows a typical TEM bright field image of the SnO_2 nanowires. The SnO_2 nanowires had a uniform diameter along their entire length. The SAED patterns were randomly taken from the SnO_2 nanowires in Fig. 3.5a, as

shown in Fig. 3.5b and 3.5c. The SAED patterns in Fig. 3.5b and 3.5c, taken from the above and below dash–line square block in Fig. 3.5a respectively, indicate that the SnO_2 nanowires preferentially grow along $[101]$ and $[1\bar{2}\bar{1}]$ directions, respectively. The TEM images are shown in Fig. 3.6 revealing the connection between a nanodendrite and a nanowire. Nanoparticles were attached together randomly forming a nanodendrite. The diameter of nanodendrites was about particle size. The sizes of the nanoparticles attaching at the nanowire were about 200 –300 nm. In contrast, the nanoparticles at an end of a nanodendrite were about 100 nm. The SAED pattern of the nanoparticles was taken from the middle of the nanodendrite as shown in the inset of Fig. 3.6b. The superimposed diffraction pattern around the main spot suggests that the nanoparticles exhibit crystalline structures. The TEM image of a leaf on a cactus–like crystal revealed that the backbone was grown in $[\bar{1}10]$ direction and the nanorods were aligned in [110] direction, as seen in Fig 3.7. Smooth facets of $<100>$ and $<010>$ planes were left at the end of the nanorods.

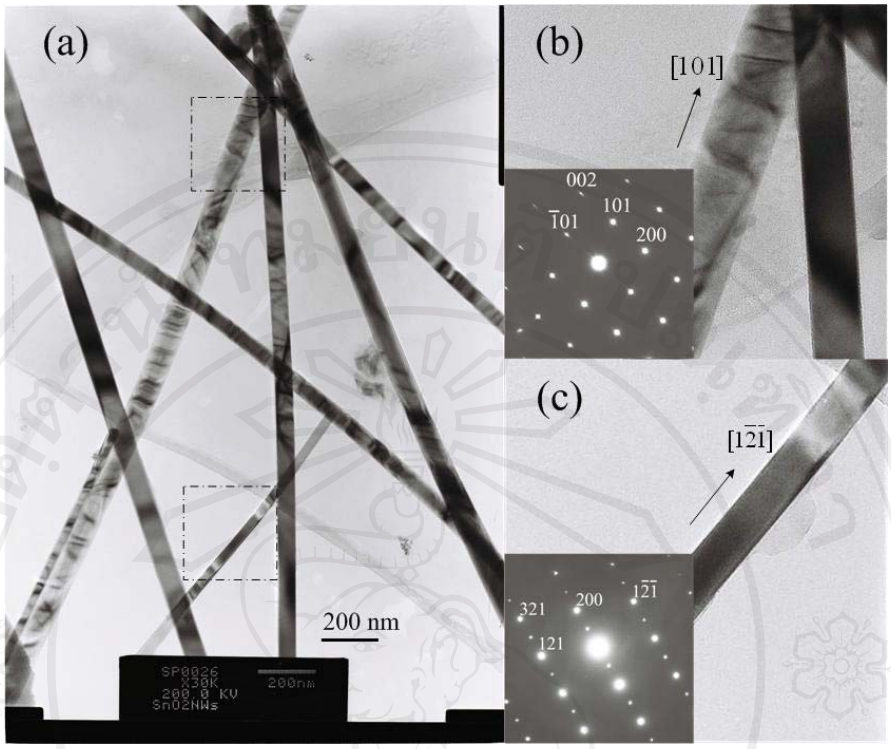

Figure 3.5 TEM image and SAED of SnO_2 nanowires

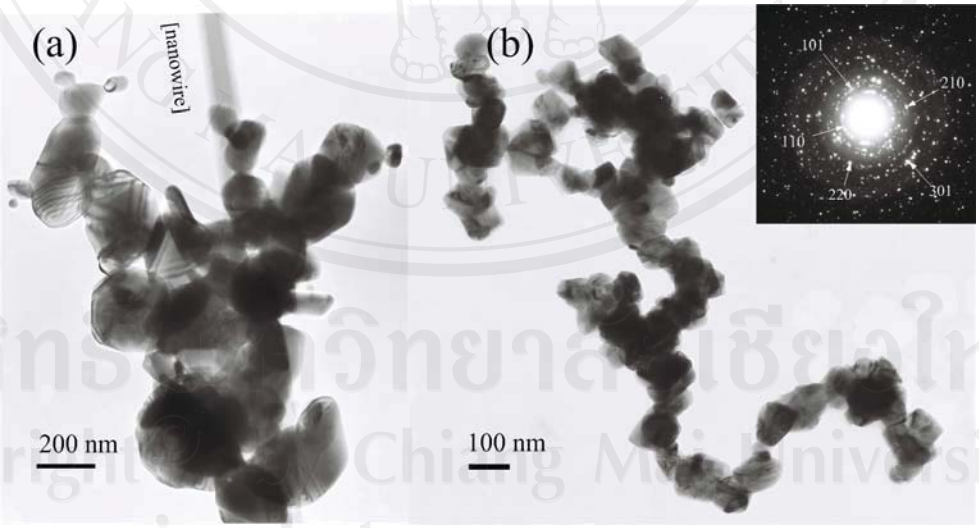

Figure 3.6 TEM images and SAED of SnO_2 nanodendrites (a) linkage of nanodendrite and nanowire (b) a nanodendrite departed from nanowire.

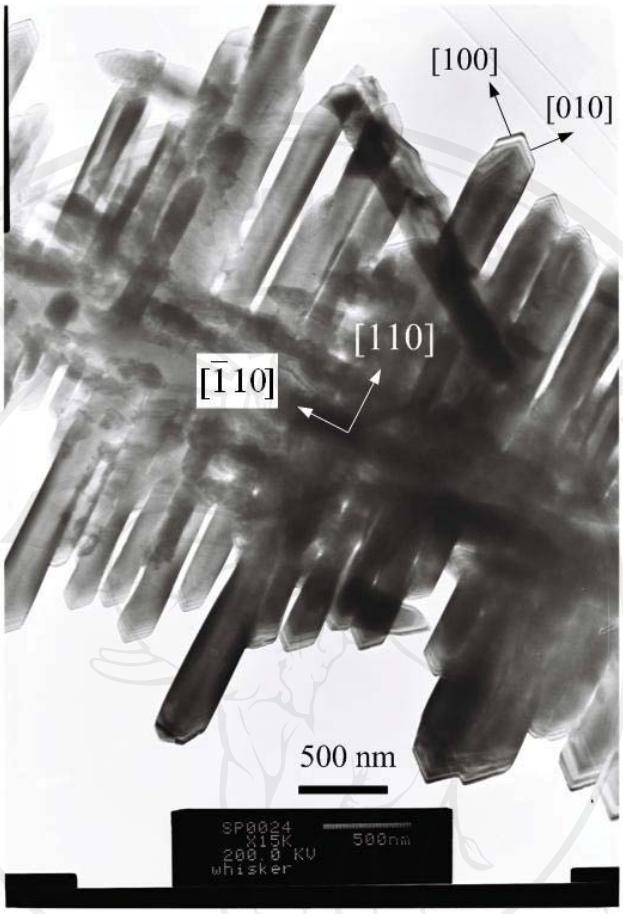

Figure 3.7 A typical TEM image of a leaf on cactus–like crystals.

3.3 Growth mechanism of SnO_2 nanostructures

Generally, the synthesis of SnO_2 nanostructures from carbothermal reduction process could be explained by using the following chemical reactions:

$$SnO_2(\text{powder}) + C(s) \rightarrow SnO(v) + CO(v) \quad (3.1)$$

$$SnO_2(\text{powder}) + CO(s) \rightarrow SnO(v) + CO_2(v) \quad (3.2)$$

$$2SnO(v) \rightarrow SnO_2(s) + Sn(l) \quad (3.3)$$

The reduction (1) and (2) can be explained by Ellingham diagram which is the plot of standard free energies for formation of oxides versus temperature [72]. The reaction incident of SnO_2 powder to SnO vapor by carbon can occur at above 700°C. Then, the CO product from the reaction (1) further reduces the SnO_2 powder as the reaction (2). The SnO (v) is metastable and will decompose to SnO_2 (s) and Sn (l) as reaction (3) [73]. Moreover, the SnO vapor possibly reacts with oxygen in the system to form SnO_2 (s). The Sn (l) can be oxidized to form SnO (v). It is also possible that the SnO_2 product can be reduced again as the reaction (1) and (2). These reactions will keep cycling until no C or CO in the system.

Considering the reaction in the loosely closed crucible system, the reductions of the SnO_2 powder occurred gradually at the bottom of the crucible when approaching 700°C and were violent when reaching 850°C. The SnO, CO, and CO_2, which were the gaseous products from the reductions of the SnO_2 powder, soared to the space above the SnO_2+C mixture and substrates. The SnO_2 product, resulting from the decomposition of the SnO (v), could be absorbed by gold droplets on the alumina substrate, leading to the formation of the SnO_2 nanowires with vapor–liquid–solid (VLS) mechanism. Therefore, the SnO_2 nanowires were grown in epitaxial directions, depending on the orientation of the seed crystal. Hence, both [101] and $[1\bar{2}\bar{1}]$ directions were observed. From our results, the SnO_2 nanowires decorated the SnO_2 nanodendrites and beaded with nanoparticles. Interesting, the mixed morphology can be achieved by utilizing the oxygen content in the system. Furthermore, for insufficiency of oxygen, SnO_2 crystals grew with no preferential direction, resulting in dendritic crystal [74]. In comparison with our work on the

mixed morphology, the SnO_2 nanowires would initially grow at early period when oxygen was adequate for the oxidation of the SnO (v) or Sn (l). The decrease of oxygen content due to the oxidation reaction and the leakage from high pressure of CO_2 leads to the insufficiency of the oxygen for the oxidation. Therefore, the SnO (v) or Sn (l) had more chance for aggregation to form particles before oxidation. The SnO or Sn particles fell to adhere randomly on the main SnO_2 nanowires. The SnO and Sn particles then gradually oxidized to be SnO_2 particles later. Consequently, the SnO_2 nanoparticles and nanodendrites could form on the surface of the main SnO_2 nanowires.

In the case more oxygen allowed to diffuse into the chamber, only microwires, microbelts, and cactus–like crystals were found. The formation of the cactus–like crystals is still unclear but probably based on VS mechanism. With closed system, amount of the oxygen is limited and CO_2 is confined in the system, acting as ambient gas to decrease the growth rate of the SnO_2 crystals. It is worth mentioning that the oxygen content could be important for the growth of the mixed morphology of the nanostructures.